

Supporting Information

A Photolabile Ligand for Light-Activated Release of Caged Copper

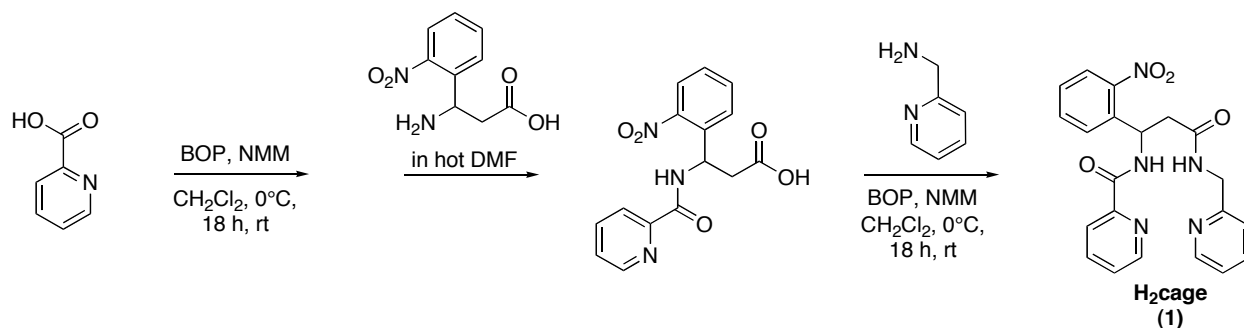
Katie L. Ciesienski, Kathryn L. Haas, Marina G. Dickens, Yohannes T. Tesema,
and Katherine J. Franz*

*Department of Chemistry, Duke University, PO Box 90346, Durham, North Carolina 27708.
Email: katherine.franz@duke.edu*

Experimental

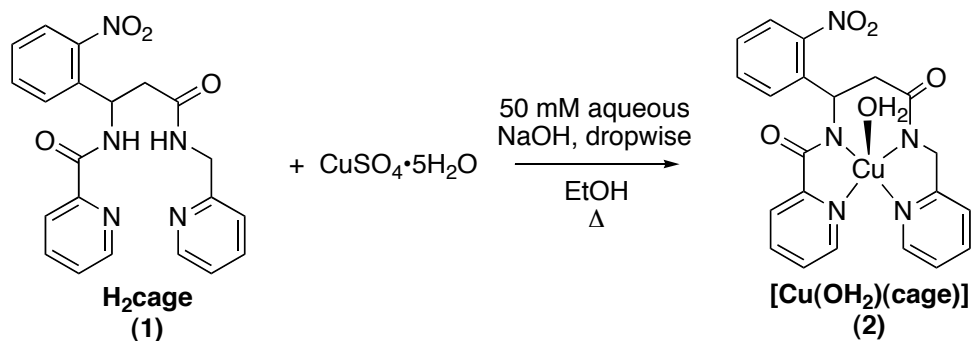
Materials and Instrumentation. All chemicals were purchased commercially and used without further purification. N-Methylmorpholine (NMM), 2-deoxy-D-ribose, ascorbic acid, 50% hydrogen peroxide, trichloroacetic acid (TCA), and 2-thiobarbituric acid (TBA) were purchased from Acros Organics; picolinic acid, 2-(aminomethyl)pyridine, picolinamide, $\text{CuSO}_4 \cdot 5\text{H}_2\text{O}$, and 1-(*o*-nitrophenyl)ethyl phosphate (cage P_i) from Sigma-Aldrich; nitrilotriacetic acid (NTA) from Fluka; 3-amino-3-(2-nitrophenyl)propionic acid from Alfa Aesar, and benzotriazol-*yloxy*tris(dimethyl-amino) phosphoniumhexafluorophosphate (BOP) from Novabiochem. All solvents were reagent grade. Chromatographic purification was carried out on basic aluminum oxide (50-200 micron) from Acros Organics. ^1H NMR and ^{13}C NMR spectra were collected on a Varian Inova 400 spectrometer with chemical shifts reported in ppm and J values in Hz. Elemental analysis was performed by Columbia Analytical Services, Inc. IR spectra were measured on a Nicolet 380 FT-IR. High-resolution, fast-atom bombardment (HR-FABMS) mass spectra were recorded on JEOL JMS-SX-102 instrument. Liquid chromatography-electrospray mass spectrometry (LC/MS) was performed using an Agilent 1100 Series apparatus with an LC/MSD trap and a Daly conversion dynode detector. A Varian Polaris C18 (150 \times 1.0 mm) column was used and peaks were detected by UV absorption at 254 nm. A linear gradient from 10% A in B to 60% A in B was run at 40 $\mu\text{L}/\text{min}$ from 2 to 18 min with a total run time of 20 min, where A is MeCN/4% 10 mM ammonium acetate buffer and B is 10 mM ammonium acetate buffer/2% MeCN. UV-vis spectra were recorded on a Cary 50 UV-vis spectrophotometer. Photolysis experiments were performed using a 1-cm pathlength screwtop quartz cuvette illuminated in a Rayonet RPR-100 Photochemical Reactor containing 16 bulbs, each 3500 Å.

Synthesis



(1) Pyridine-2-carboxylic acid {1-(2-nitro-phenyl)-2-[(pyridine-2-ylmethyl)-carbamoyl]-ethyl}-amide (H₂cage). Equimolar quantities of picolinic acid (0.100 g, 0.813 mmol) and NMM (0.089 mL, 0.813 mmol) in CH₂Cl₂ (3 mL) were added to a 50-mL round-bottom flask equipped with a stir bar. The reaction mixture was cooled over an ice bath for ten min then BOP (0.360 g, 0.813 mmol) in CH₂Cl₂ (2 mL) was added. The reaction mixture was allowed to warm to room temperature with stirring for 18 h. After 18 h, one equivalent of 3-amino-3-(2-nitrophenyl)propionic acid (0.171 g, 0.813 mmol) dissolved in hot DMF (15 mL) was added and the reaction mixture was stirred for an additional 18 h. NMM (0.089 mL, 0.813 mmol) and 2-(aminomethyl)pyridine (0.083 mL, 0.813 mmol), both in CH₂Cl₂ (3 mL) were added to the reaction mixture. The resulting solution was cooled over an ice bath for ten min then BOP (0.360 g, 0.813 mmol) in CH₂Cl₂ (2 mL) was added, and the reaction mixture stirred for 18 h at room temperature. The solvent was removed and the resulting oil was taken up in CH₂Cl₂ (25 mL), filtered, and washed with saturated aqueous NaCl solution (3 × 10 mL). The organic layers were combined, dried over MgSO₄, filtered, and solvent removal gave an oil that was purified by chromatography (basic alumina, EtOAc:hexanes, 8:2, R_f = 0.37), giving a white crystalline solid (0.220 g, 67%). ¹H NMR (CD₃OD): δ 8.69 (1H, d, *J* = 4.77), 8.42 (1H, d, *J* = 4.93), 8.03 (2H, dd, *J* = 4.65, *J* = 7.97), 7.95 (1H, td, *J* = 1.66, *J* = 7.68, *J* = 7.80), 7.74 (1H, d, *J* = 6.77), 7.61 (3H, m), 7.53 (1H, dd, *J* = 4.31, *J* = 11.17), 7.25 (1H, m), 7.17 (1H, d, *J* = 7.88),

6.08 (1H, dd, $J = 5.06$, $J = 7.09$), 4.47 (2H, dd, $J = 15.91$, $J = 42.40$), 3.11 (2H, qd, $J = 6.11$, $J = 14.80$, $J = 14.81$, $J = 14.81$). ^{13}C NMR (CDCl_3): δ 40.5, 44.1, 47.6, 122.1, 122.2, 122.5, 124.9, 126.3, 128.3, 129.1, 133.6, 137.0, 137.2, 137.3, 148.2, 148.5, 148.6, 149.6, 155.8, 164.0, 170.4; HR-FABMS: m/z 406.11 $[\text{M}+\text{H}]^+$, calcd 405.14 for $\text{M} = \text{C}_{21}\text{H}_{19}\text{N}_5\text{O}_4$; IR (MeOH, cm^{-1}): 3309, 1658, 1520, 1433, 1349, 731; UV-vis (3% MeOH in H_2O , pH 6–12), nm ($\text{M}^{-1}\text{cm}^{-1}$): 270 (8,500), 300 (1,800).



(2) $[\text{Cu}(\text{OH}_2)(\text{cage})]$. A 50 mM aqueous solution of NaOH (9.38 mL) was added dropwise to a refluxing solution of H_2cage (0.095 g, 0.234 mmol) and $\text{CuSO}_4 \cdot 5\text{H}_2\text{O}$ (0.058 g, 0.234 mmol) in 25 mL of EtOH. After refluxing for 1 h, the solvent was removed and the residue was taken up in acetone and filtered. Slow evaporation gave blue, prism-shaped crystals in 81% yield. ESI-MS: m/z 467.0 $[\text{M}+\text{H}]^+$ for $[\text{Cu}(\text{cage})]$, calcd 466.06 for $\text{C}_{21}\text{H}_{17}\text{CuN}_5\text{O}_4$; IR (neat, cm^{-1}): 1579, 1556, 1515, 1375, 1346, 1018, 755, 716, 698, 672, 647; UV-vis (H_2O , pH 6–12), nm ($\text{M}^{-1}\text{cm}^{-1}$): 580 (112); Anal. calcd. for $\text{C}_{21}\text{H}_{17}\text{CuN}_5\text{O}_4 \cdot 2\text{H}_2\text{O}$: C, 50.15; H, 4.21; N, 13.92; found: C, 51.86; H, 4.25; N, 13.97%.

Deoxyribose Assay for Hydroxyl Radical Production. The 2-deoxyribose assay was used to measure hydroxyl radical formation.¹ A mixture of copper, ascorbic acid, and hydrogen peroxide generates hydroxyl radicals by Fenton-like chemistry. Hydroxyl radicals attack 2-deoxyribose to form malondialdehyde (MDA), which upon heating with TBA under acidic conditions produces a pink chromophore ($\lambda_{\text{max}} = 532 \text{ nm}$). Chelators that prevent copper from reacting with ascorbic acid and hydrogen peroxide result in less chromophore formation. All assays were performed using 20 mM NaH_2PO_4 buffered to pH 7.4. The following reagents were added sequentially to obtain a 1 mL buffered solution with these final concentrations: chelator (10–20 μM), CuSO_4 (10 μM), 2-deoxyribose (15 mM), H_2O_2 (100 μM), and ascorbic acid (2 mM). For photolyzed samples, 500 μM solutions of $[\text{Cu}(\text{OH}_2)(\text{cage})]$ in 20 mM pH 7.4 NaH_2PO_4 buffer were photolyzed in 1-cm screwtop quartz cuvettes for 4 min in the photoreactor, then immediately diluted into the deoxyribose reaction mixtures to obtain final Cu concentrations of 10 μM . Stock solutions of CuSO_4 , ascorbic acid, and H_2O_2 were prepared fresh daily, other solutions were prepared weekly. The reaction mixtures were stirred at 37 °C for 1 h, then 1 mL of TBA (1% w/v in 50 mM NaOH) and 1 mL of TCA (2.8% w/v in water) were added. The temperature was increased to 100 °C for 20 min, then cooled to room temperature and the absorbance at 532 nm was recorded. Values are reported as A/A_0 where A_0 is the absorbance without chelator present and A is the absorbance with chelator added. The value for CuSO_4 alone is $A/A_0 = 1$. Error bars represent standard deviations from measurements done in at least triplicate.

Quantum Yield. The quantum yields of H_2cage and $[\text{Cu}(\text{OH}_2)(\text{cage})]$ photolysis were determined by comparison to the quantum yield of 1-(*o*-nitrophenyl)ethyl phosphate (cage P_i) as previously reported by Ellis-Davis and Kaplan.² Samples of H_2cage (500 μM , $A_{350} = 0.030$),

[Cu(OH₂)(cage)] (500 μM, A₃₅₀ = 0.040), or caged P_i (1 mM, A₃₅₀ = 0.065) in 20 mM NaH₂PO₄ buffer pH 7.4 in 1-mm pathlength cuvettes were irradiated in a Rayonet RPR-100 Photochemical Reactor at 350 nm for 15 s. Photodegradation of caged compounds was monitored by LC-MS analysis. Aliquots of 3.0 μL of each sample before and after photolysis were injected by autoinjector and run in triplicate. The experiment was repeated to ensure reproducibility. Comparison of the integrated peak areas indicated that after 15 s of UV exposure, 31.8% of the caged P_i, 20.0% of H₂cage, and 11.5% of [Cu(OH₂)(cage)] had been photolyzed. The quantum yield for each sample (Φ_{sample}) was calculated by using the following equation:

$$\Phi_{\text{sample}} = \Phi_{\text{cp}} \times \frac{\% \Delta_{\text{sample}}}{\% \Delta_{\text{cp}}} \times \frac{A_{350\text{cp}}}{A_{350\text{sample}}}$$

where Φ_{cp} is 0.54, the previously determined quantum yield of photolysis for caged P_i,² %Δ_{sample} and %Δ_{cp} are the percent change in integrated peak area after photolysis for the sample and caged P_i, respectively, and A₃₅₀ is the absorbance at 350 nm in a 1-mm cuvette for caged P_i (cp) and for the sample. The calculated quantum yields of photolysis for H₂cage and [Cu(OH₂)(cage)] are 0.73 and 0.32, respectively, which indicates that coordination of the ligand to Cu²⁺ decreases photolysis efficiency. In contrast, binding of Ca²⁺ in caged calcium complexes like NP-EGTA does not significantly alter the quantum yield of photolysis.² The quantum yield for H₂cage is similar to other caged compounds that release amide groups upon photolysis.^{3,4}

Potentiometric and Spectrophotometric Titrations. Cu(II) perchlorate solutions (0.1 M) were prepared from solid Cu(ClO₄)₂•6H₂O and standardized with 0.05 M EDTA to a murexide endpoint in ammonia buffer. NaOH, HClO₄, and NaClO₄ solutions (0.1 M) were prepared with boiled nanopure deionized water and were degassed upon cooling to remove dissolved

carbonate. NaOH solutions were standardized by titration with both 0.2 M HCl and potassium hydrogen phthalate to a phenolphthalein end point and were stored under Ar; HClO₄ stock solutions were prepared from concentrated perchloric acid and standardized by titration with standard NaOH to a phenolphthalein end point. All solutions were degassed with Ar for 45 minutes prior to each experimental run.

Titration were carried out at 25 °C with 0.1 M NaClO₄ supporting electrolyte in a 3-mL cuvette equipped with a pH probe, titrator tip, and stir bar, and blanketed in Ar to preserve an inert environment. The glass-bulb probe (Orion combination pH electrode model 8103BN filled with 3 M NaCl) was calibrated with pH 4 and 7 standard reference buffers (RICCA Chemical Company). Solutions of H₂cage were prepared by dissolving the compound in a minimum volume of MeOH and diluting with 0.1 M NaClO₄ in H₂O. Solutions of [Cu(OH₂)(cage)] were prepared in the range of 0.5 mM by dissolving the complex, recrystallized from methanol, in 0.1 M NaClO₄. Initial volumes were between 2 and 2.2 mL. A Schott Titronic® 110 plus autotitrator kept under constant Ar sparge was used to deliver 2 to 4 µL aliquots of acid or base through the titrator tip into the reaction cuvette. The solutions were stirred constantly and allowed to equilibrate at least 30 s after each addition before data were collected. All titrations were carried out from low to high and from high to low pH with similar results. Figure S1 shows the potentiometric titration curves of H₂cage and [Cu(OH₂)(cage)] (abbreviated as H₂L and CuL, respectively).

Titration data of the apo-ligand reveal no ionizable protons in the pH range between 2–12. This is not surprising, based on literature pK_a values of amide protons (pK_a > 20) and relevant substituted pyridine rings (pK_a < 2).⁶

Titration data for the [Cu(OH₂)(cage)] complex show two ionizable protons below pH 5. The pH-dependent spectra are shown in Figure S2. These data were fit using Specfit software

(Spectrum Software Associates, version 3.0.30) according to the model in Table S1, where β is defined by Eq. 1 for the general equilibrium reaction in Eq. 2 where $L = \text{cage}^{2-}$. The Specfit program produced $\log \beta$ values of 15.63 and 18.96 for the CuLH and CuLH_2 species respectively, which correspond to the pK_a values of 4.83 and 3.33. Attempts to include the species CuLH_{-1} , which represents the deprotonation of the coordinated water molecule in $[\text{Cu}(\text{OH}_2)(\text{cage})]$, into the model did not fit the data, indicating that this event is not observable in the tested pH range. The calculated speciation curve is shown in Figure S3.

$$\beta_{mlh} = \frac{[\text{Cu}_m\text{L}_l\text{H}_h]}{[\text{Cu}]^m[\text{L}]^l[\text{H}]^h} \quad \text{Eq. 1}$$



Table S1. Model used for the pH-dependent spectrophotometric titrations of CuL , where $L = \text{cage}^{2-}$. β is defined in Eq. 1.

Species	Log β	Cu <i>m</i>	L <i>l</i>	H <i>h</i>	
CuL	10.80 ± 0.01	1	1	0	refined
CuLH	15.63 ± 0.08	1	1	1	refined
CuLH_2	18.96 ± 0.03	1	1	2	refined
CuOH	-8.2	1	0	-1	constant ⁵
$\text{Cu}(\text{OH})_2$	-17.5	1	0	-2	constant ⁵
$\text{Cu}(\text{OH})_3$	-27.8	1	0	-3	constant ⁵
$\text{Cu}(\text{OH})_4$	-39.1	1	0	-4	constant ⁵
OH	-13.74	0	0	-1	constant ⁶

Competition study of nitrilotriacetic acid (NTA) vs. cage for Cu^{2+} . Solutions of $[\text{Cu}(\text{OH}_2)(\text{cage})]$ were prepared by dissolving $[\text{Cu}(\text{OH}_2)\text{cage}]$ that was recrystallized from methanol into 50 mM HEPES (N-(2-hydroxyethyl)-piperazine-N'-2-ethanesulfonic acid) buffer, pH 7.4, with initial concentrations ranging from 0.3–1.5 mM. The reaction vessel was a 3-mL cuvette and initial solution volumes were 1 mL. All titrations were carried out at 25 °C. Aliquots (1–2 μL) of the competitive chelator NTA (100 mM) were pipetted into $[\text{Cu}(\text{OH}_2)(\text{cage})]$ solutions and monitored spectrophotometrically. After each addition, solutions were manually mixed and equilibrated for 5 min before data were collected. A typical titration is shown in Figure S4. Data were fit to the model shown in Table S2 with Specfit software. Reported errors in $\log \beta$ were calculated from the standard deviation of three runs.

Table S2. Model for the Cu^{2+} competition study of NTA vs. L, where $\text{L} = \text{cage}^{2-}$. β is defined in Eq. 1.

Species	Log β	Cu <i>m</i>	NTA <i>l</i>	L <i>l</i>	H <i>h</i>	
CuL	10.79 ± 0.06	1	0	1	0	refined
Cu(NTA)	12.7	1	1	0	0	Constant ⁶
Cu(NTA) ₂	17.4	1	2	0	0	Constant ⁶
NTAH	9.46	0	1	0	1	Constant ⁶
NTAH ₂	11.95	0	1	0	2	Constant ¹
NTAH ₃	13.76	0	1	0	3	Constant ⁶
NTAH ₄	14.76	0	1	0	4	Constant ¹
CuOH	-8.2	1	0	0	-1	Constant ⁵

X-ray Data Collection and Structure Solution Refinement. Blue prisms of [Cu(OH₂)(cage)] were grown by slow evaporation of acetone. The crystal was mounted on the tip of a glass fiber and held in place by hardened Karo syrup. Data were collected at 296 K on a Bruker Kappa Apex II CCD diffractometer equipped with a graphite monochromator and a Mo K α fine-focus sealed tube (λ = 0.71073 Å) operated at 1.75 kW power (50 kV, 35 mA). The detector was placed at a distance of 5.010 cm from the crystal. A total of 2655 frames were collected with a scan width of 0.5° and an exposure time of 90.0 sec/frame. The frames were integrated with the Bruker SAINT v7.12A software package using a narrow-frame integration algorithm. Empirical absorption corrections were applied using SADABS v2.10 and the structure was checked for higher symmetry with PLATON v1.07. The structure was solved by direct methods with refinement by full-matrix least-squares based on F^2 using the Bruker SHELXTL Software Package. All non-hydrogen atoms were refined anisotropically. Hydrogen atoms of sp² hybridized carbons and nitrogens were located directly from the difference Fourier maps; all others were calculated. Table S3 contains a summary of crystal data, intensity collection and structure refinement parameters. Figure S5 shows the fully labeled structure with select bond distances and angles. Full lists of bond lengths and angles, atom coordinates, and anisotropic displacement parameters can be found in cif format in a separate file of Supporting Information.

Table S3. Crystal data and structure refinement for [Cu(OH₂)(cage)].

Identification code	md54
Empirical formula	C ₂₁ H ₁₉ N ₅ O ₅ Cu
Formula weight	484.95
Temperature	296(2) K
Wavelength	0.71073 Å
Crystal system	Monoclinic
Space group	P2(1)/n
Unit cell dimensions	a = 7.7037(4) Å α = 90 ° b = 12.2546(8) Å β = 95.364(3) ° c = 21.0831(12) Å γ = 90 °
Volume	1981.6(2) Å ³
Z	4
Density (calculated)	1.625 Mg/m ³
Absorption coefficient	1.149 mm ⁻¹
F(000)	996
Crystal size	0.12 x 0.05 x 0.04 mm ³
Crystal color and habit	Blue prism
Diffractometer	Bruker Kappa Apex II
Theta range for data collection	1.92 to 24.96°
Limiting indices	-9<=h<=8, -14<k<=14, -25<=l<=25
Reflections collected	30154
Independent reflections	3429 [R(int) = 0.0815]
Completeness to theta = 24.96	98.9 %
Absorption correction	Semi-empirical from equivalents
Max. and min. transmission	0.9555 and 0.8744
Solution method	SHELXS-97 (Sheldrick, 1990)
Refinement method	SHELXL-97 (Sheldrick, 1997)
Data / restraints / parameters	3429 / 0 / 293
Goodness-of-fit on F ²	1.152
Final R indices [I>2σ(I)]	R1 = 0.0410, wR2 = 0.0983
R indices (all data)	R1 = 0.0664, wR2 = 0.1093
Largest diff. peak and hole	0.773 and -0.333 e·Å ⁻³

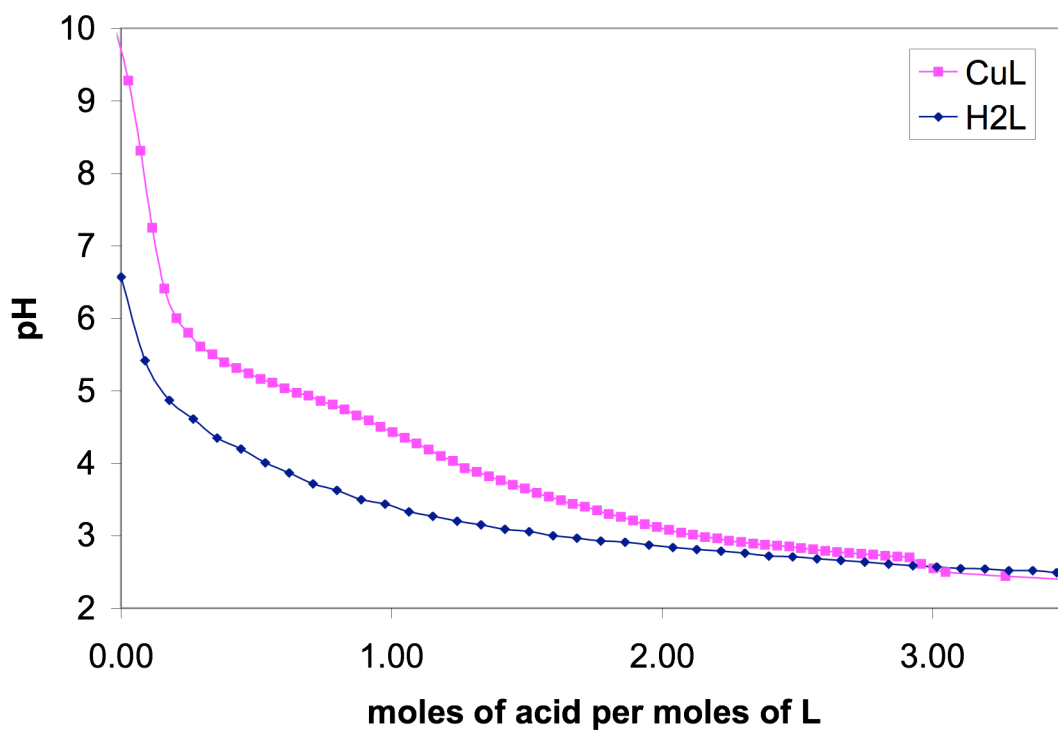


Figure S1. Potentiometric titration curves of H_2L (blue diamonds, $[\text{L}] = 1.46 \text{ mM}$) and CuL (pink squares, $[\text{CuL}] = 1.33 \text{ mM}$), where $\text{L} = \text{cage}^{2-}$. $T = 25 \text{ }^\circ\text{C}$, $\mu = 0.1 \text{ M NaClO}_4$.

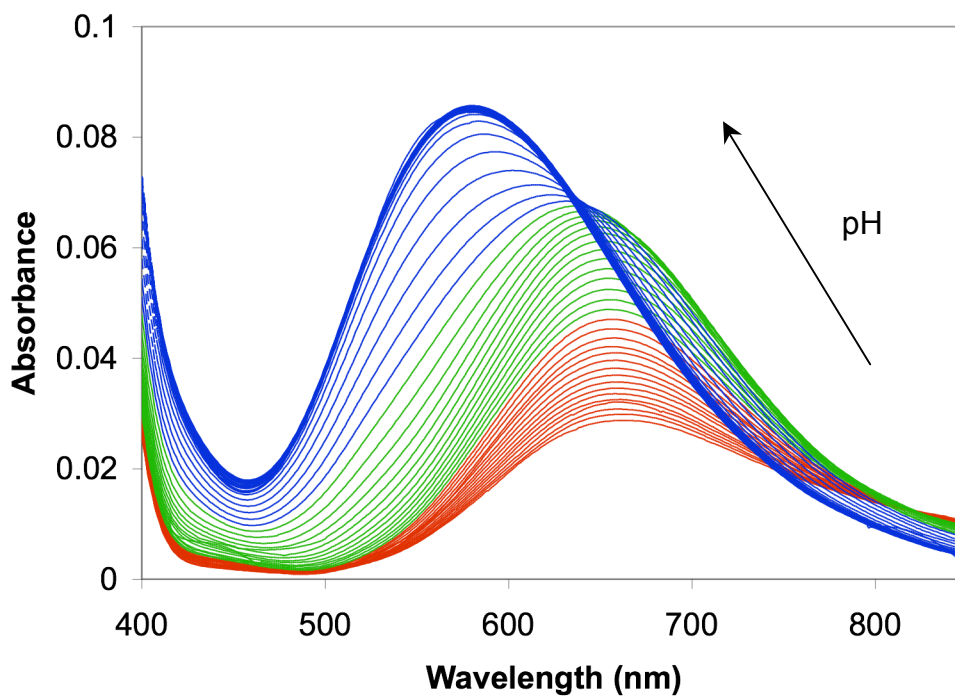


Figure S2. pH-Dependent spectrophotometric titration of $[\text{Cu}(\text{OH}_2)(\text{cage})]$ from pH 2.7 to 12. $T = 25 \text{ }^\circ\text{C}$, $[\text{Cu}] = [\text{cage}] = 0.71 \text{ mM}$, $\mu = 0.1 \text{ M NaClO}_4$.

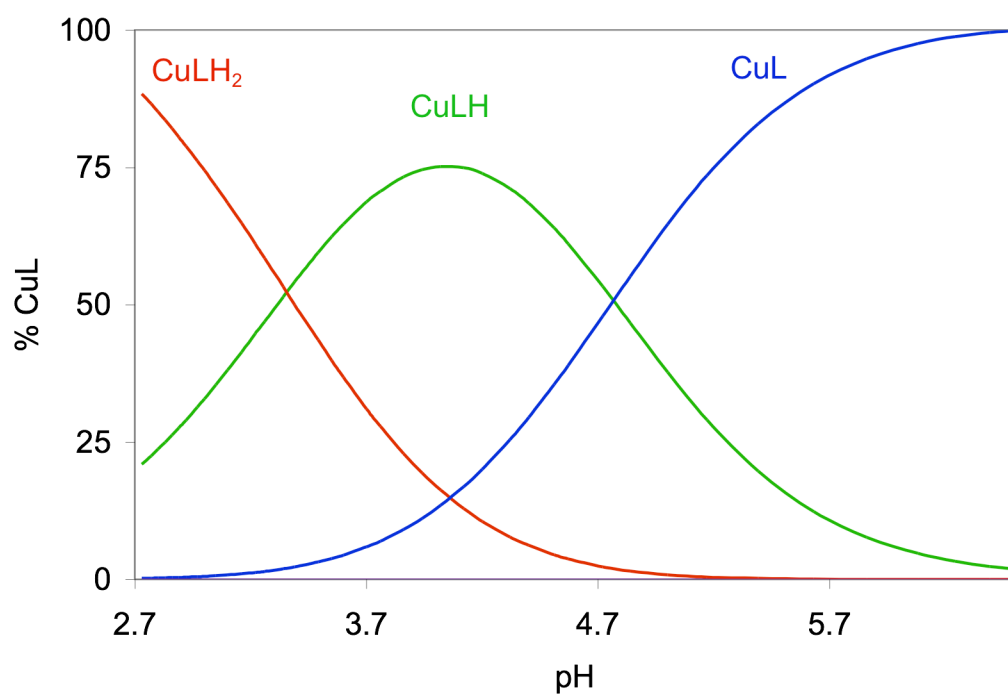


Figure S3. Calculated species distribution for Cu^{2+} complexes of L, where $\text{L} = \text{cage}^{2-}$. Conditions as described in Figure S2.

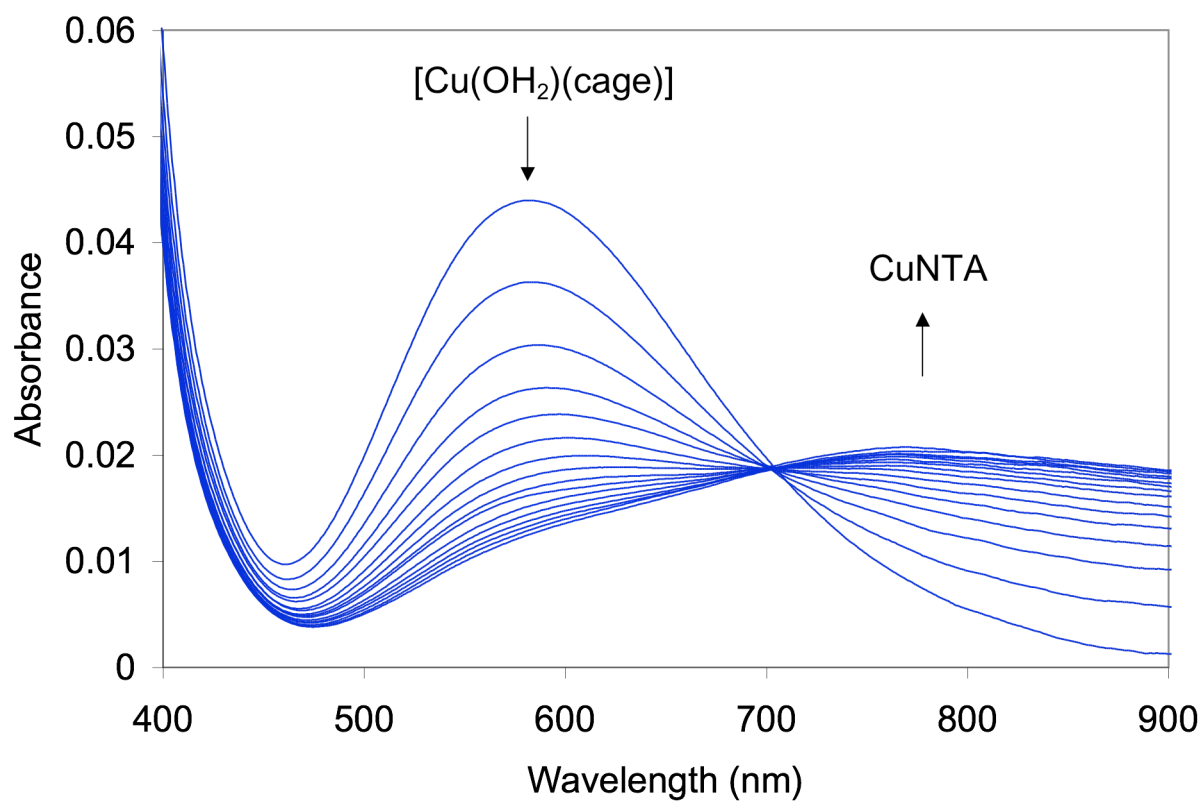


Figure S4. Titration of NTA into a 0.39 mM solution of $[\text{Cu}(\text{OH}_2)(\text{cage})]$ in 50 mM HEPES buffer.

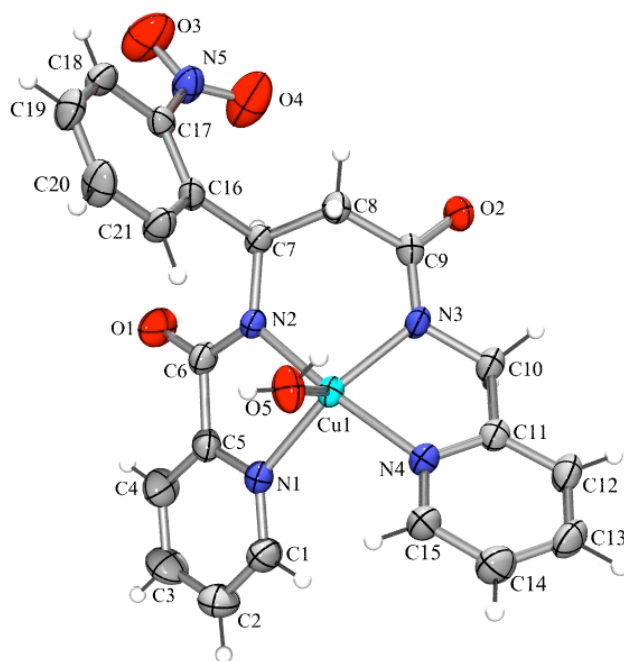


Figure S5. ORTEP diagram of $[\text{Cu}(\text{OH}_2)(\text{cage})]$ showing 50% thermal ellipsoids. Selected bond distances: Cu–N1, 2.052(2); Cu–N2, 1.948(3); Cu–N3, 1.943(3); Cu–N4, 2.013(3), Cu–O5, 2.295(3) Å. Distance between the ortho H's on C1 and C15 (H1–H15), 2.4955 Å. Selected bond angles: N2–Cu–N4, 172.8(1); O5–Cu–N3, 117.0(1); O5–Cu–N1, 100.9(1); N1–Cu–N3, 141.9(1); N2–Cu–N3, 92.9(1); N3–Cu–N4, 80.8(1); N1–Cu–N4, 100.7(1); N2–Cu–N1, 82.1(1); N2–Cu–O5, 100.8(1); O5–Cu–N4, 85.3(1)°.

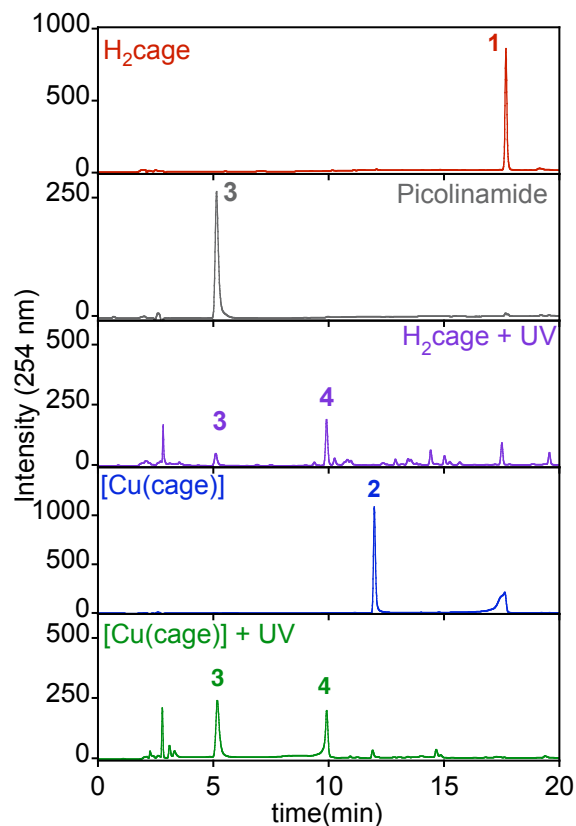


Figure S6. Chromatography traces for H₂cage (**1**), standard picolinamide (**3**), [Cu(cage)] (**2**), and [Cu(cage)] + UV are shown in the main text but repeated here to compare to the trace for H₂cage after 4 min of exposure to UV light (H₂cage + UV), which gives major photolysis products **3** and **4**. For each run, 6 μ L of a 100 μ M solution in phosphate buffer of H₂cage or photolyzed H₂cage (or 3 μ L of 500 μ M for the Cu-containing samples and picolinamide) were injected onto the LC/MS. Mass spectra extracted from the ion chromatograms that are associated with these LC traces are shown in Figure S7.

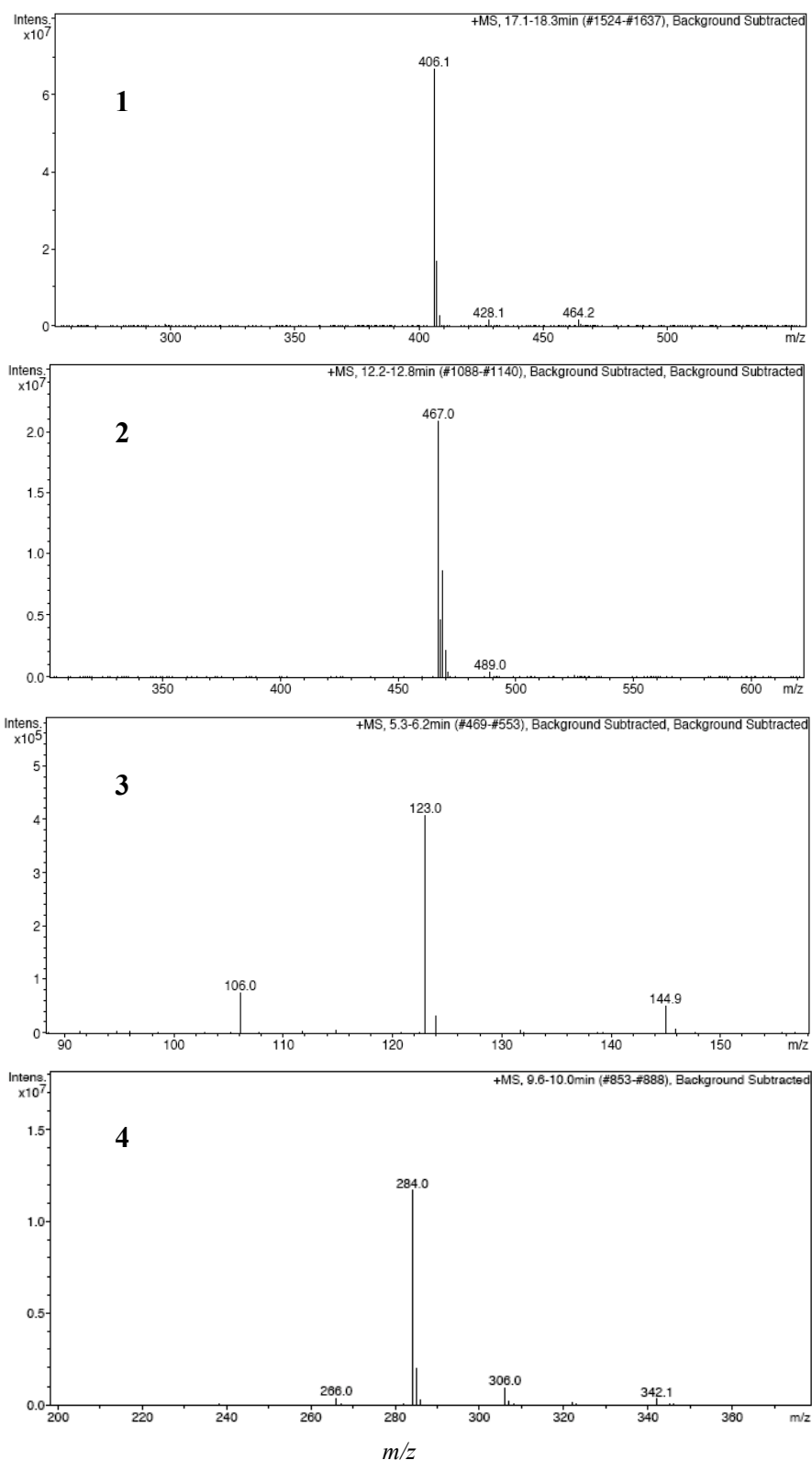


Figure S7. Positive-mode mass spectra extracted from the ion chromatograms associated with the LC traces in Figure S6. Primary ion values of m/z are calculated in all cases for $m = (M+H^+)$ and $z = 1$. **1** is H_2cage eluting ~ 18 min, calcd: 406.15, found: 406.1; **2** corresponds to $[Cu(cage)]$ eluting ~ 12 min, calcd: 467.12, found: 467.0; **3** is picolinamide ~ 5 min, calcd: 123.06, found: 123.0; and **4** is the nitroso-containing photoproduct that elutes ~ 10 min, calcd 284.11, found: 284.0.

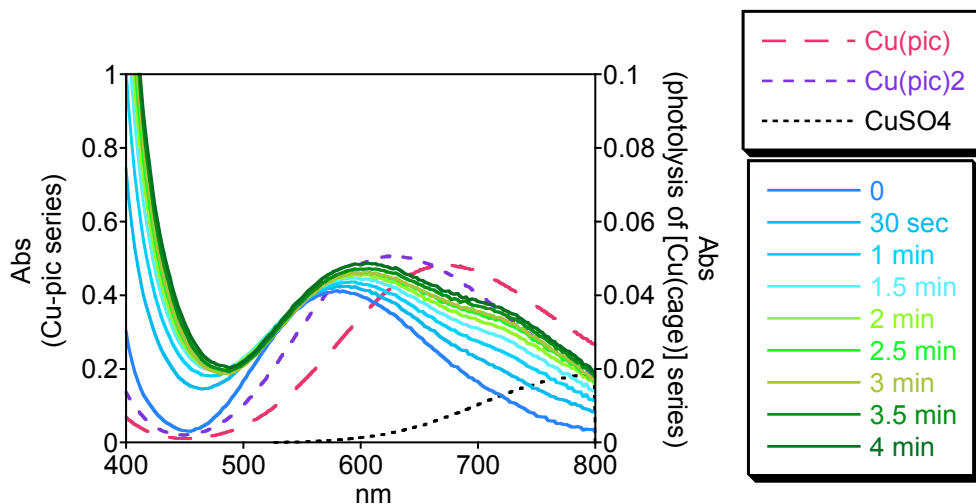


Figure S8. Absorption spectra showing the changes in the Cu^{2+} d-d region for a $350\ \mu\text{M}$ solution of $[\text{Cu}(\text{OH}_2)(\text{cage})]$ in $20\ \text{mM}$ NaH_2PO_4 buffer pH 7.4 ($t = 0$) following 30 sec intervals of photolysis for a total of 4 min of UV exposure. The spectra of CuSO_4 alone and in the presence of one and two equiv of picolinamide are also shown for comparison.

References

- ¹ Halliwell, B.; Gutteridge, J. M. C.; Aruoma, O. I. *Anal. Biochem.* **1987**, *165*, 215-219.
- ² Ellis-Davies, G. C. R.; Kaplan, J. H. *Proc. Natl. Acad. Sci. U.S.A.* **1994**, *91*, 187-191.
- ³ Wieboldt, R.; Ramesh, D.; Jabri, E.; Karplus, P. A.; Carpenter, B. K.; Hess, G. P. *J. Org. Chem.* **2002**, *67*, 8827-8831.
- ⁴ Milburn, T.; Matsubara, N.; Billington, A. P.; Udgaonkar, J. B.; Walker, J. W.; Carpenter, B. K.; Webb, W. W.; Marque, J.; Denk, W.; Mccray, J. A.; Hess, G. P. *Biochemistry* **1989**, *28*, 49-55.
- ⁵ Kragten, J. *Atlas of Metal-Ligand Equilibria in Aqueous Solution*; Ellis Horwood: New York, 1978.
- ⁶ Martell, A. E.; Smith, R. M. In *NIST Standard Reference Database 46*; 6.0 ed.; Motekaitis, R. J.; NIST: Gaithersburg, MD, 2001.

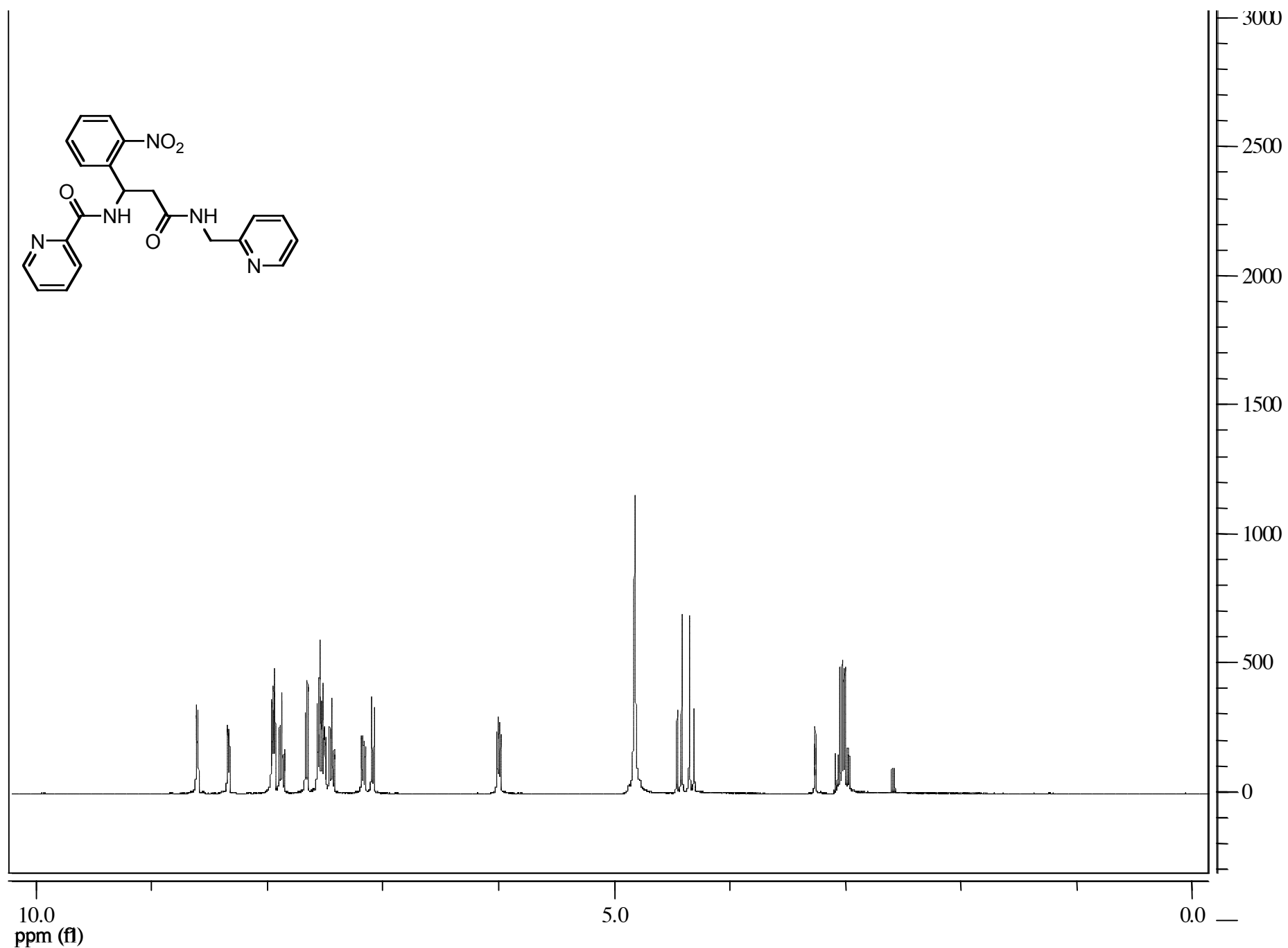


Figure S7. ^1H NMR spectrum of H_2cage in CD_3OD . The peak at δ 2.67 is due to residual hexamethylphosphoramide (HMPA) generated during amide bond formation, and accounts for less than 0.7% of the product.

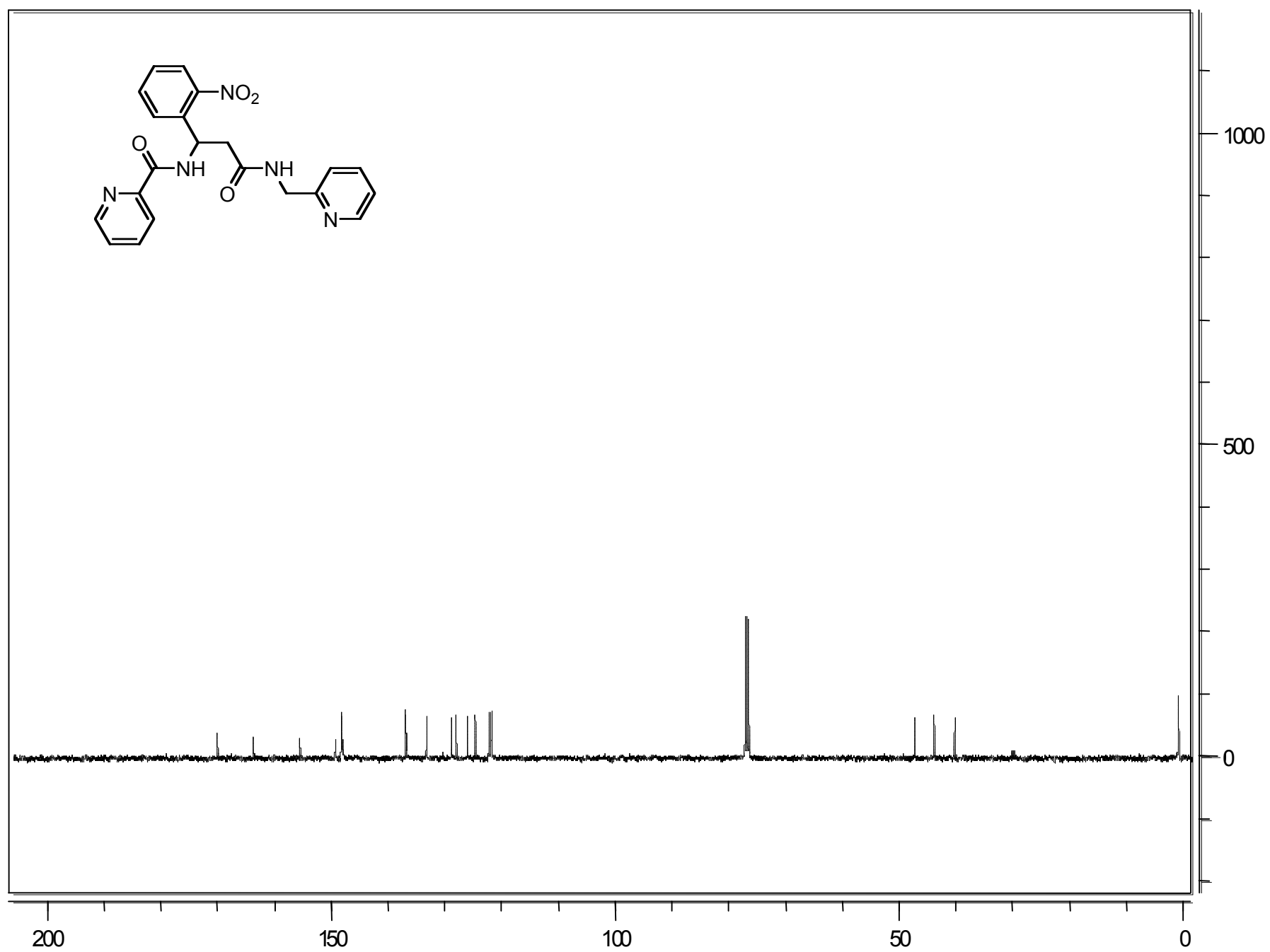


Figure S8. ^{13}C NMR spectrum of H_2cage in CDCl_3 .